ISSN 0036-0244, Russian Journal of Physical Chemistry A, 2017, Vol. 91, No. 13, pp. 2636–2642. © Pleiades Publishing, Ltd., 2017.

PHYSICAL CHEMISTRY OF NANOCLUSTERS AND NANOMATERIALS

DFT Theoretical Calculation of the Site Selectivity of Dihydroxylated (5, 0) Zigzag Carbon Nanotube[1]

H. Mostaanzadeh*, A. Abbasi*, and E. Honarmand

Department of Chemistry, University of Qom, Qom, Iran

**e-mail: h.mostaan@qom.ac.ir*

Received June 16, 2016

Abstract—Functionalization is an important method to change electrical and thermodynamic properties of carbon nanotubes. In this study, the effect of functionalization of a single-walled carbon nanotube (SWCNT) was investigated with the aid of density functional theory. For this case, a (5, 0) zigzag SWCNT model containing 60 C atoms with 10 hydrogen atoms added to the dangling bonds of the perimeter carbons was used. To model hydroxyl CNT two terminal H atoms were replaced by two –OH groups. All the functionalized CNTs are thermodynamically more stable and have higher dipole moment with respect to the pristine CNT. Depending on the positions of hydroxyl groups on CNT five isomers of $C_{60}H_8(OH)_2$ were obtained. The structure of these five isomers and molecular properties such as the HOMO–LUMO gaps, the dipole moments, and the density of state were calculated. Our results indicate that the HOMO–LUMO gap strongly depends on the placement of the hydroxyl groups on the nanotubes. The isomers were hydroxyl groups locate on the anti-position show the highest distortions in the structure of the CNT.

Keywords: carbon nanotube, ab initio calculation, hydroxyl functionalization, site selectivity

DOI: 10.1134/S0036024417130155

1. INTRODUCTION

Carbon nanotubes (CNTs) have attracted the interest of scientists and engineers since their discovery in 1993 [1], due to their unique structural, mechanical, and electronic properties and large application potential [2–5]. Carbon nanotubes have significant potential for application in molecular electronics [6, 7], nanomechanics [8], optics [9], sensors [10], and catalysis [11]. Single-wall carbon nanotubes (SWCNT) are frequently referred to as one-dimensional structures because of their nanoscale dimensions and quantum properties. Rational design of advanced composite materials requires some kind of interaction between SWCNT and the surrounding matrix. Acids are used for cleaning and removing remaining metal catalyst introduced to raw carbon nanotube (CNT) material in the process of their synthesis. Consequently, SWCNTs that are functionalized at their ends (rims) by COOH or –OH groups are formed [12]. Two types of SWCNT functionalization sidewall and end functionalization are known and have been studied experimentally and theoretically [13, 14]. The functionalization of pristine SWCNTs dramatically changes their chemical, electronic and transport properties [15]. Molecular modeling of structure and energetic, in particular at the density functional theory (DFT) level, provides in material sciences a fairly efficient and inexpensive way of support for future laboratory studies.

The present work is a theoretical study of end-substituted zigzag SWCNTs with two –OH groups. Full-geometry optimizations are performed on the (5, 0) pristine and functionalized SWCNT using DFT calculations. Thermodynamic possibility of functionalizing on one or two ends of the tube with –OH substituents and properties of the resulting isomers have been studied.

2. MODEL AND COMPUTATIONAL METHODS

In this study, we used a (5, 0) zigzag carbon nanotube with 60 C atoms as SWCN model. Ten hydrogen atoms saturated the dangling bonds of both sides in the pristine CNT. The functionalized models were obtained by replacing two H atoms by hydroxyl groups at different positions to get five structural isomers as shown in Fig. 1.

In order to obtain the lowest energy level (true ground state), the ground state geometries of the single-walled carbon nanotubes (SWCNTs) and the functionalized-SWCNTs (f-SWCNTs) were optimized without symmetry restriction on the initial structures. All the calculations were performed using density functional theory (DFT) and B3LYP (Becke Three Parameter) Hybrid Functional, in which the

[1] The article is published in the original.

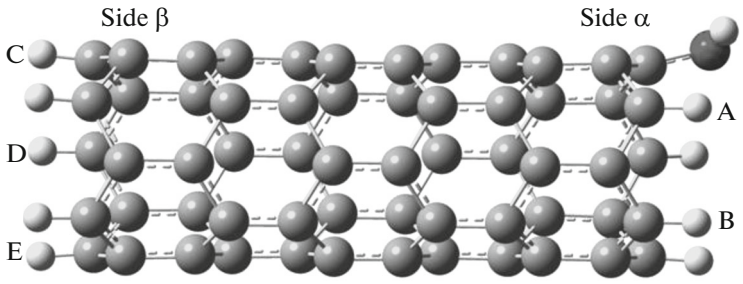

Fig. 1. Model of (5, 0) zigzag CNT with 60 C atoms which is used in this study; A–E represent the different positions of the second substituted –OH with respect to the first one which is dominate in this figure.

exchange functional is the Becke's three parameter type, including gradient correction, and the correlation correction involves the gradient-corrected functional of Lee, Yang and Parr [16]. This method was chosen because it is computationally less demanding than the other approaches as regards the inclusion of electron correlation and it has shown to successfully predict a wide range of molecular properties. The basis set used is 6-31G(*d*), as implemented in the Gaussian 03 software package [17]. The results of the calculations did not produce any imaginary frequencies. The vibrational mode descriptions were made on the basis of the calculated nuclear displacements using visual inspection of the animated normal modes using the GaussView03 software [18].

3. RESULTS AND DISCUSSION

3.1. Thermodynamic Aspects

All structures, including non-functionalized CNT are fully optimized using B3LYP/6-31G(*d*) level of theory. Supposing the hydroxyl-functionalized CNTs are produced from the following reaction.

$$C_{60}H_{10} + O_2 \rightleftharpoons C_{60}H_8(OH)_2.$$

The reaction Gibbs free energy in the standard condition (ΔG°) were obtained as:

$$\Delta G^\circ = G^\circ_{CNT(OH)_2} - G^\circ_{CNT} - G^\circ_{O_2}, \quad (1)$$

where $G^\circ_{CNT(OH)_2}$, G°_{CNT}, and $G^\circ_{O_2}$ are the standard Gibbs free energies of hydroxylated CNTs, original CNT, and O_2, respectively, which are obtained at the theory level discussed previously.

The last column of Table 1 represents the reaction Gibbs free energies of hydroxylated CNTs were obtained using Eq. (1). The negative values of ΔG for these structures reveal the reactions of CNT with O_2 are highly favorable with high percent of production from the thermodynamic point of view. However, the variances from –489.6 to –500.4 kJ mol^{-1} reveal the site selectivity of hydroxyl groups in the reaction of oxygen with CNT. Among all the hydroxylated isomers, the structure C which two –OH groups are located at two terminals of CNT at the syn position (Fig. 1) shows the lowest value for ΔG (–500.4 kJ mol^{-1}). Inconsistently, the structure A with –489.6 kJ mol^{-1} value for ΔG is thermodynamically less stable with the lowest percent of production. Therefore, in the production of hydroxylated CNT from reaction (1) structure C is the most abundant product.

3.2. Geometries, Dipole Moments, and Frontier Orbital Energies

The geometries of all OH–CNTs are highly modified regarding to the original CNT due to the bonding of –OH groups to the terminals C atoms of the CNT. The cross sections of hydroxylated CNTs are not cir-

Table 1. Orbital energies for HOMO, LUMO, HOMO–LUMO gaps (ΔE), dipole moments (μ), Gibbs free energies (G°) of compounds and reaction Gibbs free energies of all hydroxylated compounds obtained in the gaseous phase*

Comp.	E_{HOMO} (eV)	E_{LUMO} (eV)	ΔE (eV)	μ (D)	G° (kJ/mol)	ΔG° (kJ/mol)
A	–3.610	–2.852	0.758	1.7013	–6410597.8	–489.65
B	–3.675	–2.828	0.847	3.1290	–6410605.2	–497.05
C	–3.657	–2.882	0.775	1.9963	–6410608.5	–500.35
D	–4.199	–2.912	1.287	5.6604	–6410605.0	–496.85
E	–4.206	–2.867	1.339	5.6293	–6410604.8	–496.65
CNT	–3.761	–2.979	0.782	0.3643	–6409957.9	

* Using B3LYP/6-31G(*d*) theory level.

Table 2. Geometrical parameters of optimized structures of CNTs major and minorax is of the cross section of the CNT inlets; α represents the inlet where is closer to –OH groups and β represents the inlet which is farther from hydroxyl groups; δ is the distance between the minor and the major axis. All data are reported in Å

Compound	Side α			Side β		
	minor diameter	major diameter	δ_d	minor diameter	major diameter	δ_d
A	3.72246	3.99219	0.2697	3.60434	3.97187	0.3675
B	3.76718	3.89809	0.1309	3.56712	4.0000	0.4329
C	3.68360	3.97668	0.2931	3.68331	3.97751	0.2942
D	3.74728	3.81078	0.0635	3.17625	4.13830	0.9620
E	3.68285	3.90195	0.2191	3.17451	4.13754	0.9630
CNT	3.57789	3.98969	0.4119	3.57789	3.98969	0.4119

cular. Instead, they have elliptical shapes. The ellipses major and minor axis of both inlets and the difference between them (δ_d) which are reported in Table 2 reveal the degree of deformation in the structure of CNTs due to the CNT hydroxylation. When two hydroxyl groups locate in anti-position (D and E isomers), CNT perform highest deformation with respect to the original CNT and the structure C where two –OH groups locate at the syn-position shows lowest deformation even from the regular CNT (Fig. 2).

The data in Table 1 show that all molecular properties such as frontier orbital energies, gapes between E_{HOMO} and E_{LUMO} (ΔE) and the electrical dipole moments (μ) strongly depend to the positions of hydroxyl groups. The band gap energies (ΔE), electrical dipole moments (μ) and deformation patterns (δ_d) of all studied structures, which are reported in Tables 1, and 2 are depicted as diagrams in Fig. 3. This figure shows that ΔE and μ obviously relate to the δ_d and it is interesting that the structures D and E, which have the higher geometrical deformation, represent higher values for ΔE and μ. The shapes of HOMO and LUMO orbitals which are shown in Fig. 4 are also related to the positions of the –OH groups. This object nicely can be seen in the structures A and B that –OH groups are in the same side or D and E which –OH are in anti-positions of different sides. In structure C where –OH groups are located in the syn-position of two different sides, the frontier orbitals show a kind of fine symmetric configuration.

The direction and the relative magnitude of the electrical dipole moments also are shown in Fig. 4. Like the other molecular properties, dipole moments are strongly depend on the hydroxyl group positions. From the higher electronegativity of O atoms with respect to C atoms, we expect that the magnitude of μ in the structures that two –OH are in one side (A and B), would be higher than the structures that two hydroxyl groups are in two sides. In fact, the results in Fig. 4 are contradictory to our first expectation while, the magnitude of μ in A and B is smaller than D and E. We also are not able to predict the direction of the

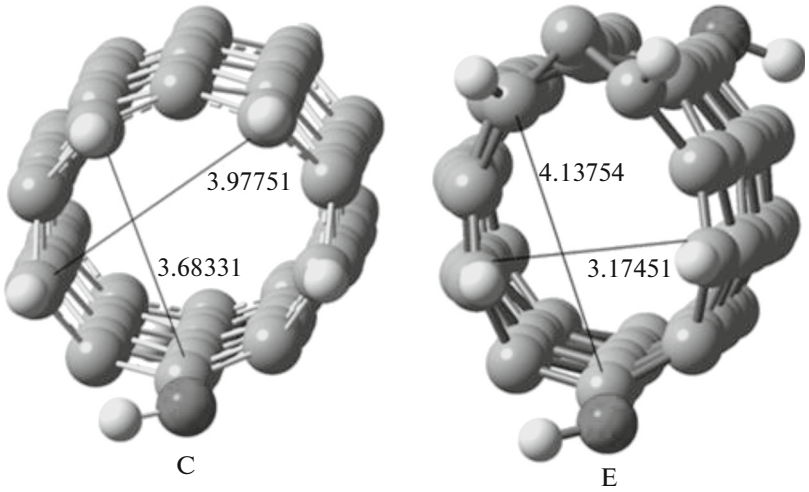

Fig. 2. The schematic view of the inlet cross section of C and D, the lines represent major and minor axes of the elliptical cross sections.

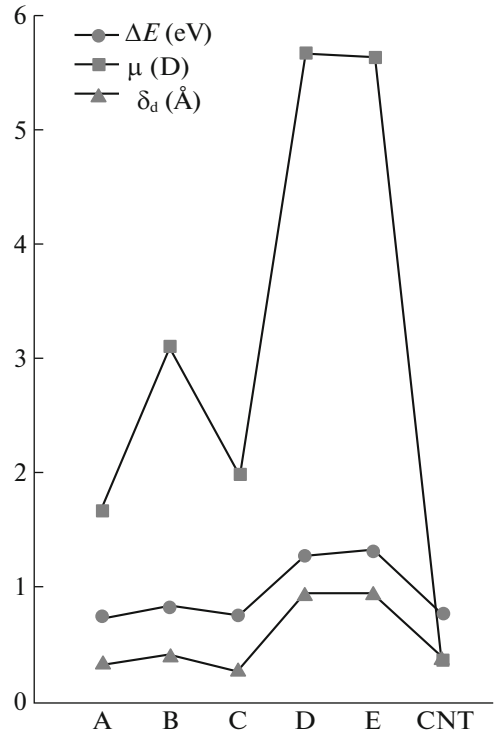

Fig. 3. Comparison of the band gap energies (ΔE), electrical dipole moments (μ), and deformation patterns (δ_d) of all studied structures.

dipole moments vectors from the positions of –OH. For instance, in the structures D and E, the direction of the dipole moments are toward to the inlets with the higher δ_d or in C which δ_d of both inlets are relatively identical, the direction of μ vector is perpendicular to the longitudinal of the CNT. Therefore, we conclude that, the CNT deformation plays the main role in the magnitude and the direction of the dipole moments in these structures.

3.3. IR Spectra of Hydroxylated CNT

The calculated IR-spectra of the structures A–E including pristine CNT are shown in Fig. 5. The strongest vibrational modes, which are represented in Table 3, reveal that the IR vibrational frequencies depend to the positions of –OH on the CNT. Except, the IR spectra of D and E, all the other structures have similar IR spectra. For instance, the global breathing modes (which appear in fingerprint area) in the pristine CNT and A–C do not see in D and E. moreover, the stretching vibrational frequencies of both –OH groups in A–C are overlapped and appear in one frequency, whereas these frequencies are separated in D and E as shown in Fig. 6. Similar differences can be seen in the C–H stretching vibrational frequencies, which present in lower frequencies in D and E with respect to the other structures. Other vibrational frequencies such as C=C stretching and bending modes do not depend too much on the position of hydroxyl groups

3.4. Density of States (DOS)

DOS "which describes the number of states per interval of energy at each energy level that are available" is a nice parameter that normally uses for the evaluation of electrical conductivity and optical properties of systems. Figure 7 shows the DOS of CNT and all hydroxylated CNT. The obtained values of the band gap (ΔE) that are reported in Table 1 as well as the DOS diagrams in Fig. 7 can be used to qualify the electrical conductivity. Two parameters are important for this qualification. One is the values of the band gap

Table 3. The strongest vibrational mode of structure A–E and the pristine structure; the notation ν is used for the stretching and δ for the bending vibrational normal modes; $\delta_{(C-H)^{\perp}}$ represents the bending vibrational model of C–H groups which vibrate in perpendicular to the longitude side of CNT

	Norm. mod	$\nu_{(C-O)}$	$\nu_{(C=C)}$	$\nu_{(O-H)}$	$\nu_{(C-H)}$	$\delta_{(C-H)^{\perp}}$	$\delta_{(O-H)}$
A	freq	1339–1372	1504–1612	3706	3184–3204	875	1331, 1335
	intens	266.4	180.8	123.7	34.1	227.9	54.7
B	freq	1375	1505–1603	3717	3185–3251	898	1430
	intens	249.8	168.9	170.0	26.6	220.0	253.0
C	freq	1349, 1377	1501–1614	3712	3185–3227	876	1338
	intens	529.5	189.0	114.1	38.6	188.0	43.8
D	freq	1368–1378	1519–1602	3691, 3716	3144–3230	886	1282, 1306
	intens	133.0	114.2	196.8	129.0	63.6	109.7
E	freq	1368, 1379	1504–1603	3692, 3713	3143–3222	886	1273–1319
	intens	363.7	122.2	198.9	128.4	51.3	82.5
CNT	freq	–	1501–1598	–	3189–3207	897	–
	intens	–	281.6	–	40.4	329.2	–

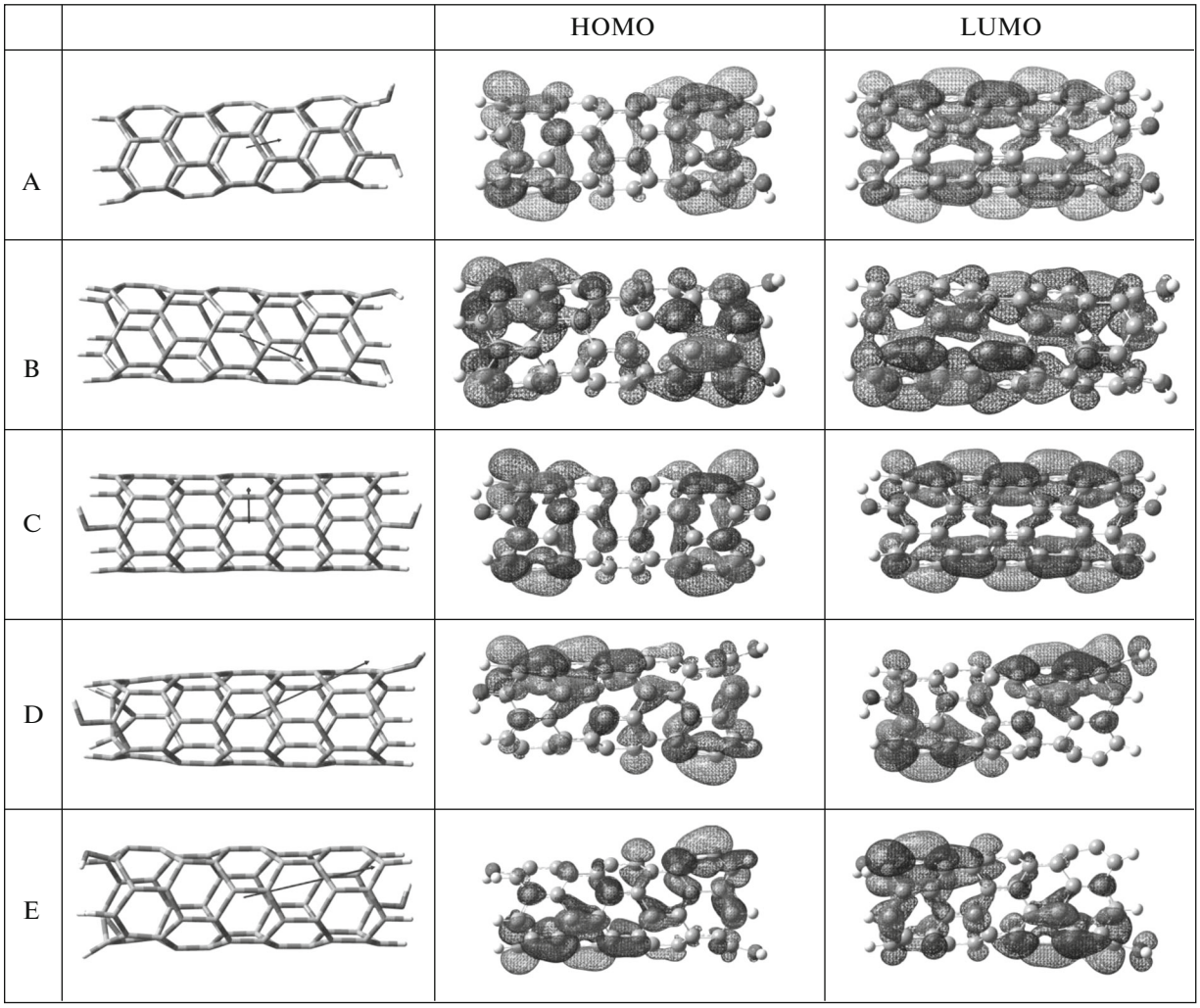

Fig. 4. Optimized geometries and the shapes of HOMO and LUMO molecular orbitals of 5 isomers of $C_{60}H_{10}(OH)_2$ using B3LYP/6-31G(*d*) theory level. Arrows represent the attitude and the size of dipole moments.

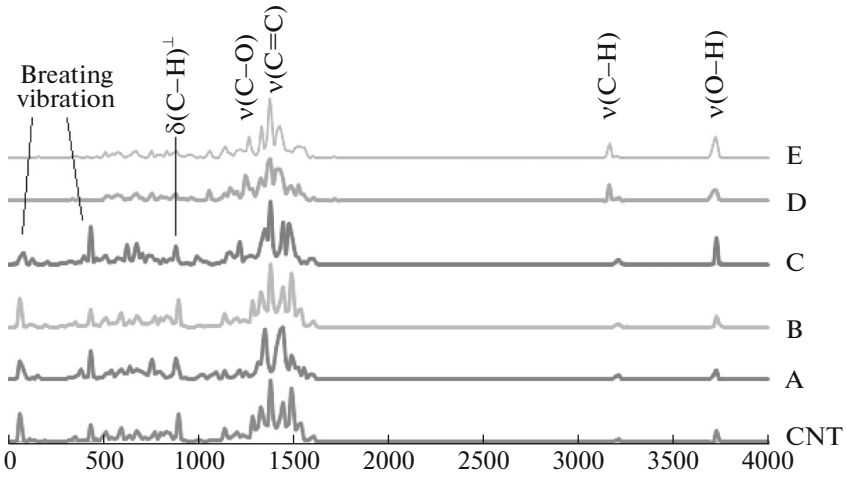

Fig. 5. IR spectra of structure A–E and C_6OH_{10} CNT obtained using UB3LYP/6-31G(*d*) theory level. The notation ν is used for stretching and δ for bending vibrational normal modes.

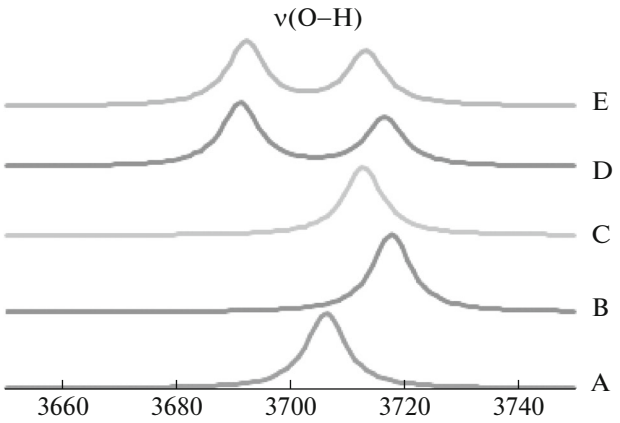

Fig. 6. Stretching vibrational frequency of –OH (ν_{OH}) of all the studied isomers.

and the other is the shape of DOS. For instance, D and E, which have the higher band gap in the comparison with other structures, would be less conductive. A–C have ΔE in the range or even smaller than the pristine CNT band gap (for structures A and C). Although these structures have almost the same values for ΔE, but A–C perform higher electrical conductivity than CNT while, the conductive bands in the structures A–C are continuous contradictory to that of the CNT.

The general conclusion here is that the positions of hydroxyl groups influence a lot on the electrical properties of structures.

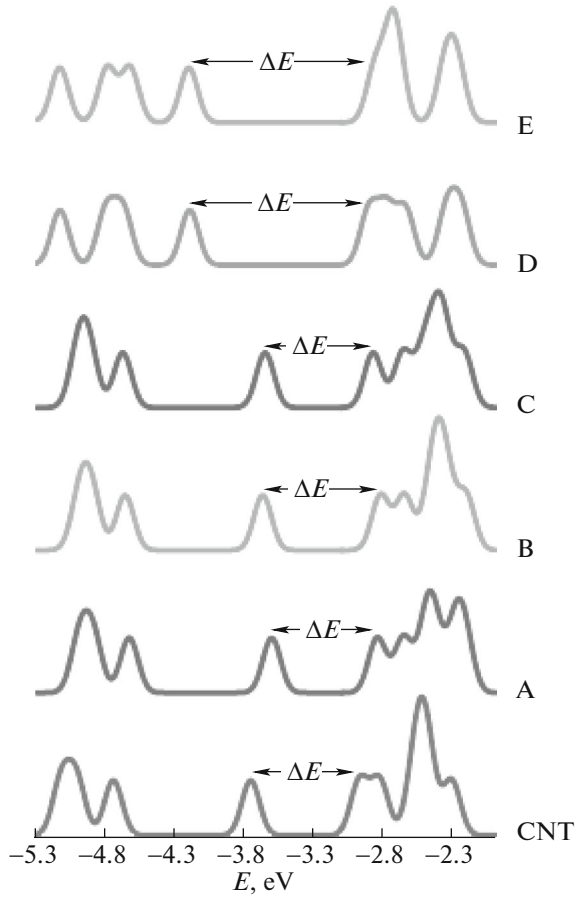

Fig. 7. DOS of A–E isomers in the range of frontier orbital energies (–5.3 to –2.0 eV).

4. CONCLUSIONS

In this study the structure of different isomers of dihydroxylated CNT have been studied using DFT calculations. For this purpose a (5, 0) zigzag CNT with 60 C atoms have been used. Two –OH groups were replaced by the two terminal hydrogens that were used to saturate dangling bonds. All the five possible structures of $C_{60}H_8(OH)_2$ were optimized and analyzed in detail. These calculations show all the molecular properties such as geometry, stability, vibrational frequencies, and electrical properties strongly depend on the position of hydroxyl groups. In structures D and E where –OH groups are located in anti-positions on both sides of CNT present properties, which are highly differ from the other studied structures. For instance, these two structures have higher dipole moments and band gaps. The IR spectra and DOS of them are also do not the same as the others. In the structure C where –OH groups are located on two sides, but in the syn-position, we observe higher electrical conductivity and symmetrical geometry than the other related isomers even than CNT.

ACKNOWLEDGMENTS

The authors would like to acknowledge the financial support of University of Qom and Iranian National Committee of Nanotechnology in Ministry of Science, Research, and Technology.

REFERENCES

1. S. Iijima, Nature **354**, 56 (1991).
2. A. Minett, F. Schüth, S. W. Sing, J. Weitkapmp, K. Atkinson, and S. Roth, in *Handbook of Porous Solids* (Wiley-VCH, Weinheim, 2002).
3. Z. Yao, H. W. C. Postma, L. Balents, and C. Dekker, Nature **402**, 273 (1999).
4. O. Zhou, H. Shimoda, B. Gao, S. Oh, L. Fleming, and G. Yue, Acc. Chem. Res. **35**, 1045 (2002).
5. R. H. Baughman, C. Cui, A. A. Zakhidov, Z. Iqbal, J. N. Barisci, G. M. Spinks, G. G Wallace, A. Mazzoldi, D. de Rossi, A. G. Rinzler, O. Jaschinski, S. Roth, and M. Kertesz, Science **284**, 1340 (1999).
6. N. Ferrer-Anglada, V. Gomis, Z. El-Hachemi, U. D. Weglikovska, M. Kaempgen, and S. Roth, Phys. Status Solidi **203**, 1082 (2006).

7. Z. Chen, J. Appenzeller, Y. M. Lin, et al., Science **311**, 1735 (2006).
8. D. A. Britz and A. N. Khlobystov, Chem. Soc. Rev. **35**, 637 (2006).
9. Y. Sakakibara, A. G. Rozhin, H. Kataura, Y. Achiba, and M. Tokumoto, Jpn. J. Appl. Phys. **44**, 1621 (2005).
10. M. E. Kose, B. A. Harruff, Y. Lin, L. M. Veca, F. Lu, and Y. P. Sun, J. Phys. Chem. B **110**, 14032 (2006).
11. P. Serp, M. Corrias, and P. Kalck, Appl. Catal. A **253**, 337 (2003).
12. M. V. Veloso, A. G. S. Filho, J. M. Filho, S. B. Fagan, and R. Mota, Chem. Phys. Lett. **430**, 71 (2006).
13. T. Kar, B. Adkim, X. Duan, and R. Pachter, ChemPhysLett. **423**, 126 (2006).
14. C. G. Salzmann, S. A. Llewellyn, G. Tobias, M. H. Y. Ward, Y. Huh, and M. L. H. Green, Adv. Mater. **19**, 883 (2007).
15. J. Zhao, J. P. Lu, J. Han, and C. K. Yang, Appl. Phys. Lett. **82**, 3746 (2003).
16. A. D. Becke, J. Chem. Phys. **98**, 5648 (1993).
17. M. J. Frisch et al., *Gaussian 03, Revision E.01* (Gaussian Inc., Wallingford, CT, 2004).
18. *Gaussview 03* (Gaussian Inc., Wallingford, CT, 2003).